Insights from scanning tunneling microscopy experiments into correlated electron systems

Benschop, T.

Chapter 5

Noise enhancement in the tunneling current between an STM tip and Sr_2IrO_4

We observe noise enhancements in the tunneling current when scanning a Sr_2IrO_4 sample. These appear to be highly localized, but do not appear to correlate strongly with any feature in the local density of states. The existence of substantial random telegraph noise (RTN) in addition to shot noise can explain the noise spectra we observe. Fitting our data with a model results in characteristic frequencies of ~ 100 GHz. We believe these noise enhancements indicate polaron formation in Sr_2IrO_4.

5.1 Introduction

Sometimes nature surprises us. This is applicable to many phenomena everywhere, but this work is supposed to be centered around condensed matter physics, and so in this chapter, we will limit ourselves to a material with chemical formula Sr_2IrO_4. A material that behaves as a metal, yet at low temperatures, becomes insulating and shows similarities to the famous high-Tc superconductor family of copper oxides, or cuprates.
Sr_2IrO_4 has a perovskite crystal structure, and belongs to a broader group of materials we refer to as "iridates". This work is on the n = 1 Ruddlesden-Popper phase, which hosts a Mott insulating state at low temperatures. From now on, if we refer to iridates, we refer to this n = 1 phase.
By substitution of Sr atoms with La, these materials can be chemically doped during their growth. For this reason, the material originally attracted a lot of attention as a candidate testbed for Mott physics, specifically the effects of doping on a Mott insulator. In the cuprates, a wide range of exotic electronic states of matter is revealed after doping the parent (Mott insulator) material [9]. The questions are to what degree these phenomena originate from Mottness, or if they are rooted in a different cause. Doping a (chemically different) Mott insulator can hopefully provide us with more insights in this matter. Important here is also the dissimilarity in doping: where cuprates are mainly hole doped through introduction of excess oxygen, iridates are electron doped through substitution of Sr atoms with La.
Upon doping iridates, at around $\sim 5\%$ La substitution, a pseudogap is revealed in the density of states (DOS) [135]. This phenomenology has a striking resemblance to the cuprates, where a pseudogap state also emerges from the doped Mott state. Unfortunately, unlike the cuprates, iridates have never been shown to superconduct. The problem here is that it is hard to achieve the theoretically required doping level, as only a finite number of Sr atoms can be substituted, and dopants tend to cluster together. Electrostatic doping on the other hand is complicated due to the relatively large number of free carriers in the material [136].
The interpretation of this pseudogap phase has been a long standing topic in condensed matter physics. The fact that similar phenomenology is observed both in cuprates and in iridates is striking, and hints at some degree of universality regarding the origin of this kind of superconductivity in Mott physics. One hypothesis about the pseudogap phase is that it is some sort of precursor state to superconductivity, where Cooper pairs are already present, but due to phase fluctuations, a coherent condensate can not be formed giving rise to the observed spectral gap without bulk superconductivity. This hypothesis remains to be verified, and one tool that could be of great importance here is noise spectroscopy. If Cooper pairs already exist in the pseudogap state, it is possible that they contribute to Andreev like tunneling processes, which would be detectable by noise spectroscopy measurements [137]. This is one of the reasons why we attempted noise spectroscopy measurements on iridates here.
Another motivation for noise measurements on iridates is its Mott physics. In a Mott insulator, electron transport is governed by hopping, One could imagine that this can lead to irregularities when we are trying to pull electrons out of the material, in our

case with the STM tip. The hopping rate from site to site can be lower then the rate at which electrons tunnel to the tip, leading to charging effects that should be detectable as shot noise deviations from its normal Poissonian value.
Thus, we decided to attempt to measure shot noise on an iridate sample.

5.2 STM on Sr_2IrO_4

We study a La doped iridate sample (10%) with our home-built liquid He 4 system containing our MHz amplifier (chapter 4, [129,138]). The crystal is cleaved *in-situ* at 4.2 K after which it is loaded directly into the STM head. In figure 5.1, we present our results. Figure 5.1a shows a typical topography obtained in a 30 nm field of view. La dopants are visible as dark atoms with a bright square around them. In the same field of view, we perform STM spectroscopy, measuring the local density of states at each pixel.

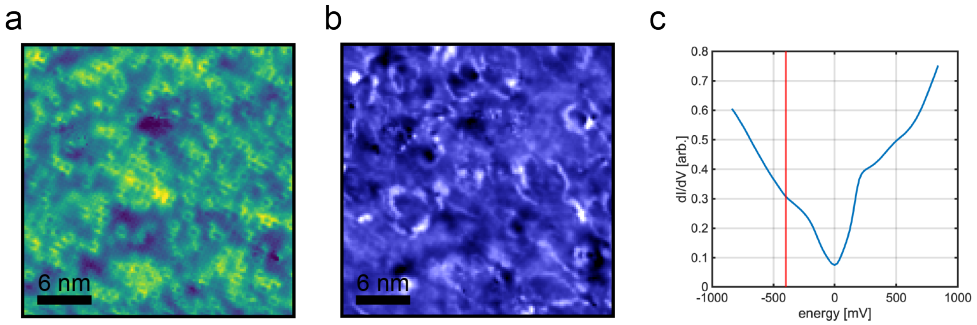

Figure 5.1: STM results
a) Topography of the iridate surface measured in a 30 nm field of view (V = -840 mV , I = 300 pA). La dopants appear as dark sports with a bright square around. b) Spectroscopic map layer with V = -400 mV in the same field of view as (a). c) Average conductance spectrum measured in the same field of view as (a).

Figure 5.1b shows the energy layer with V = -400 mV. We can see bright, ring shaped features which are induced by the STM tip. This phenomenon is better known as tip induced band bending, or TIBB, and in well known to occur in these samples [135,139], but is also well known in semiconductor studies with STM [140].
In the simplest way, we can describe TIBB as local electrostatic gating. Iridates have a relatively high number of free carriers compared to for example graphene. Compared to copper, however, the free carrier density is actually relatively low [136]. Because of this, the electric field that emanates from the STM tip is not fully screened and is finite at the surface of the crystal. When the STM tip moves across the sample, the field induces some extra charge underneath the tip shifting spectral features in apparent energy. Around impurities with strongly localized states, this results in the ring shapes observed [141].
In figure 5.1c, we plot the average conductance spectrum measured in the field of view

of 5.1b. This spectrum strongly resembles the pseugogap-like spectra measured in reference [135], consistent with the doping level of 10%.

5.3 Noise measurements

We continue by presenting our noise spectroscopy measurements on different locations close to La dopants on the sample. Starting in figure 5.2b, we measure shot noise in a small bias range around the Fermi level, with a junction resistance of 200 MΩ. Interestingly, both for positive and negative bias, we observe multiple noise enhancements at -57, -46.5, 19.5, 36, and 54 mV respectively. We measure each side of the spectrum multiple times in order to test reproducibility. Each individual measurement is presented with a different color. The noise shows the same noise enhancement at similar energies each time, demonstrating these features are robust.
In different locations, we observe no clear noise enhancement figure 5.2c,d, figure 5.3, implying that the observed phenomenon is location dependent.
At higher energies, we also measure substantial noise enhancement, as shown in figure 5.2e,f. In this location, noise is enhanced around -300 and 450 mV respectively. Note that on the positive side of the spectrum, for low bias, enhancement is also measured yet these low bias features seem absent for negative energies in this location.

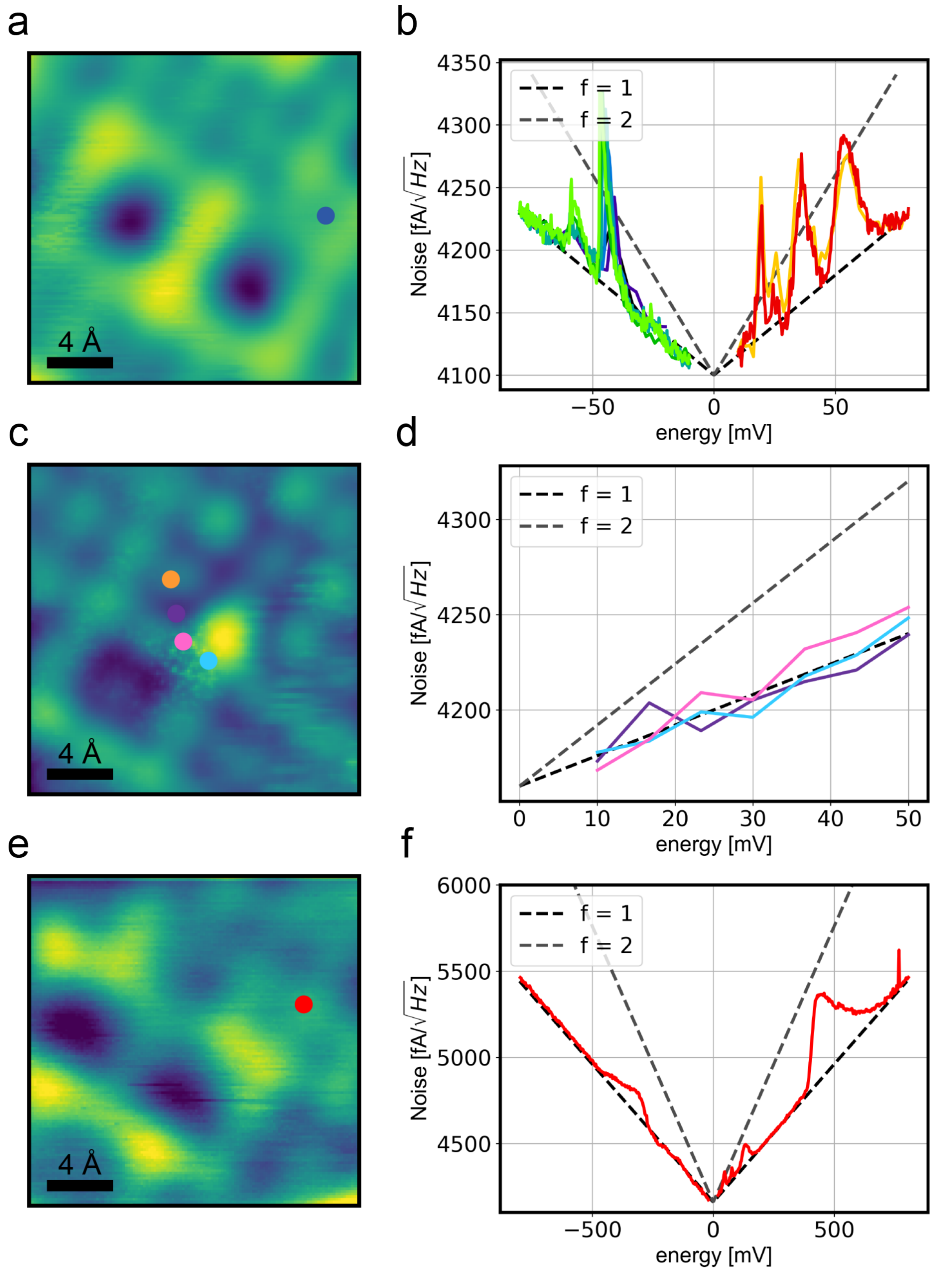

Figure 5.2: Noise measurements at different locations
In the left column, a dot indicates the position of the noise measurement displayed in the right column. For figure (c) and (d), the color of the line corresponds to the color of the dot indicates the location of the measurement. Data taken at the location with the orange dot is presented in figure 5.3. Each measurement was done with a junction resistance of 200 MΩ. The dashed lines indicate Poissonian noise (f = 1) and doubled Poissonian noise (f = 2).

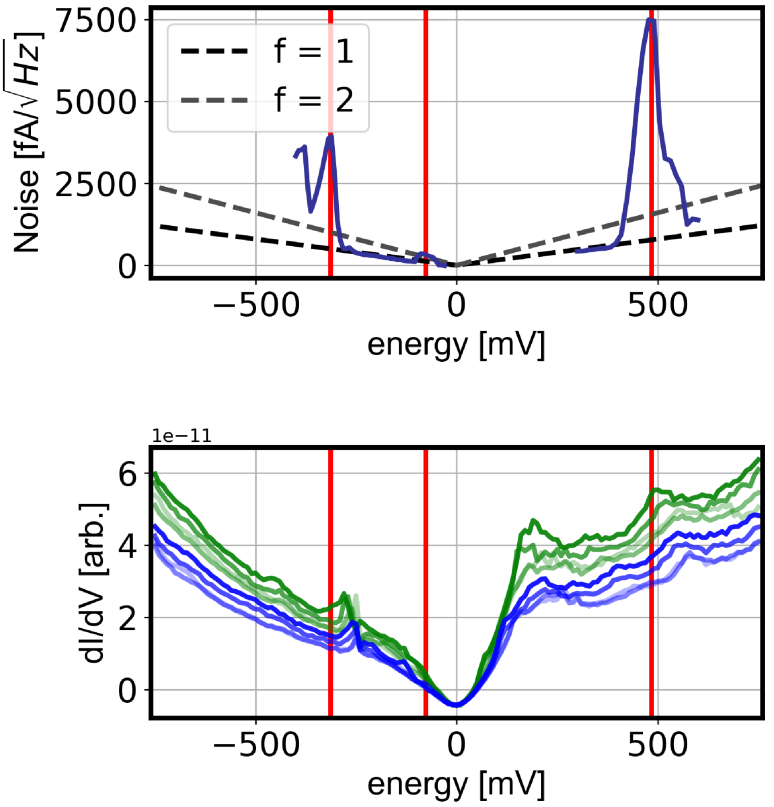

Figure 5.3: Comparing noise- and local DOS spectra
In the panel on top, we show a noise spectrum measured at the location marked with an orange dot in figure 5.2c, with a junction resistance of 200MΩ. The dashed lines indicate Poissonian noise (f = 1) and doubled Poissonian noise (f = 2). In the bottom panel, local DOS measurments at the same location are plotted, measured with different initial conditions (blue: I = 4 nA, green: I = 5 nA; V = 750, 850, 950, 1000 mV, high to low color intensity).

In order to gain some insight about the origin of these noise enhancements, we perform spectroscopy measurements at the location marked by an orange dot in figure 5.2c. Noisy impurities can give rise to noise enhancement [142, 143], so a good first step is maybe to look for features in the local DOS at energies where the noise enhancement is observed. In figure 5.3, we show noise spectra and local DOS measurements in the same locations. Local DOS measurements are performed with different setup conditions (see figure caption), because of the present TIBB effect. Unfortunately, the DOS does not exhibit very sharp spectral features, yet is is intriguing how some noise enhancements do seem to coincide with kinks in the local DOS. In particular the outermost measured enhancements at -314 and 484 mV respectively. This, however, does not appear convincing enough to attribute the observed enhancement to a particular impurity state.

5.4 Random telegraph noise

In the previous section, we reported highly localized spots with noise enhancement on the surface of the iridate sample. The question is still, what is the origin of these spots? Although we have not observed these on a standard surface, *e.g.* the gold (111) surface, we are not sure at this point if these spots are really intrinsic to the iridates, or if this could be some sort of switching state on our tip, or maybe even a combination of both, where the tip influences the state in the iridate crystal. It could be that the iridates provide a base for this enhancement to occur, for example due to its poor electronic screening causing a rather inhomogeneous electric field at the surface.
Although we cannot definitively determine the origin of these observed noise enhancements, we speculate about a scenario where the noise we measure is not exclusively shot noise, but rather a combination of shot- and random telegraph noise (RTN). This was proposed earlier in the context of magnetic tunnel junctions [144]. RTN, or popcorn noise as it is also sometimes referred to, occurs when a system fluctuates between 2 or more levels. In the context of STM, RTN is sometimes observed in the tunneling current when the tip is unstable. The electronic state at the end of the tip changes rapidly, resulting in sharp, sudden jumps in the measured tunneling current.
According to reference [145], the power spectrum of a fluctuating 2 level system is given by:

$$S_{V,RTN}(f) = S_0 \frac{\tau_{eff}}{1 + (2\pi f \tau_{eff})^2}, \tag{5.1}$$

where $S_0/4$ is the integrated power, τ_{eff} is an effective time constant associated with the transition between the levels and f is the measurement frequency. We rewrite this equation :

$$S_{V,RTN}(f) = A \frac{f_c}{f^2 + f_c^2}, \tag{5.2}$$

where $A = \frac{S_0}{2\pi}$, and $f_c = \frac{1}{2\pi\tau_{eff}}$ is the characteriestic frequency of the fluctuations. We assume that this characteristic frequency is proportional to some thermal activation function. We model this as:

$$f_c = f_0 e^{-\frac{E}{V}}, \tag{5.3}$$

where E is a parameter specifying the activation energy, f_0 is the attempt frequency of the 2 level and V is the applied voltage. When can further modify the expression to accommodate the electric field of our tip. For now, we limit ourselves to a shift of the voltage linear in junction resistance R, and scaled with some proportionality constant k. This results in the following expression:

$$f_c = f_0 e^{-\frac{E}{V-kR}} \tag{5.4}$$

Because the current noise, S_I, is equal to $S_I = S_V/R^2$, we can use equation 5.1 and 5.4 to model our measured data. The measured noise, $S_{I,Total}$, is determined as:

$$S^2_{I,Total} = S^2_{I,shotnoise} + S^2_{I,RTN}, \tag{5.5}$$

where the shot noise term is given by the well known expression
$S_{I,shotnoise} = 2e\langle I\rangle$, where $\langle I\rangle$ is the time averaged current, and e the elementary charge.
We test this model on the data presented in figure 5.2b. We focus on the negative side of the spectrum. Our results are displayed in figure 5.4.
The noise spectrum in figure 5.4a shows two distinct peaks. In order to be able to fit our model to the data, we split the spectrum in 2 sections, roughly in the middle between the two noise enhancement peaks. In figure 5.4b-d, the blue dots indicate the data points in the subsection that is being analyzed.
Starting with the noise peak around -57 mV, we see that our model fits the data rather well. Continuing with the noise enhancement around -46.5 mV, we see that the shape of this peak is a bit different from that of the previous one. On the right hand side of the peak, it appears as if there is a small shoulder. Indeed, simply trying to fit this data with the model was not possible, however, what we observe here could be a result of two peaks that are very close together in energy. Indeed, fitting 2 peaks close to each other seems to reproduce the observe peak shape quite good (figure 5.4d). The total peak fit (red) is composed of the green- and purple peaks shown in the figure.

The origin of the RTN is unfortunately very difficult to determine. The fit results give characteristic frequencies around ~ 100 GHz. In the cuprates, noise centers have previously been observed, and attributed to the formation of polarons in the chemical buffer layers [146]. Here, charge is trapped for macroscopic time scales explaining the large c-axis resistivity of cuprates. Although the chemical makeup of cuprates and iridates is radically different, polaronic excitations are also known to occur in iridates [147–149]. Therefore, although the noise enhancements observed here are less strong then in the case of the cuprates, we believe the physics that governs these is similar.
Earlier, we briefly mentioned noisy impurities as an alternative explanation for our

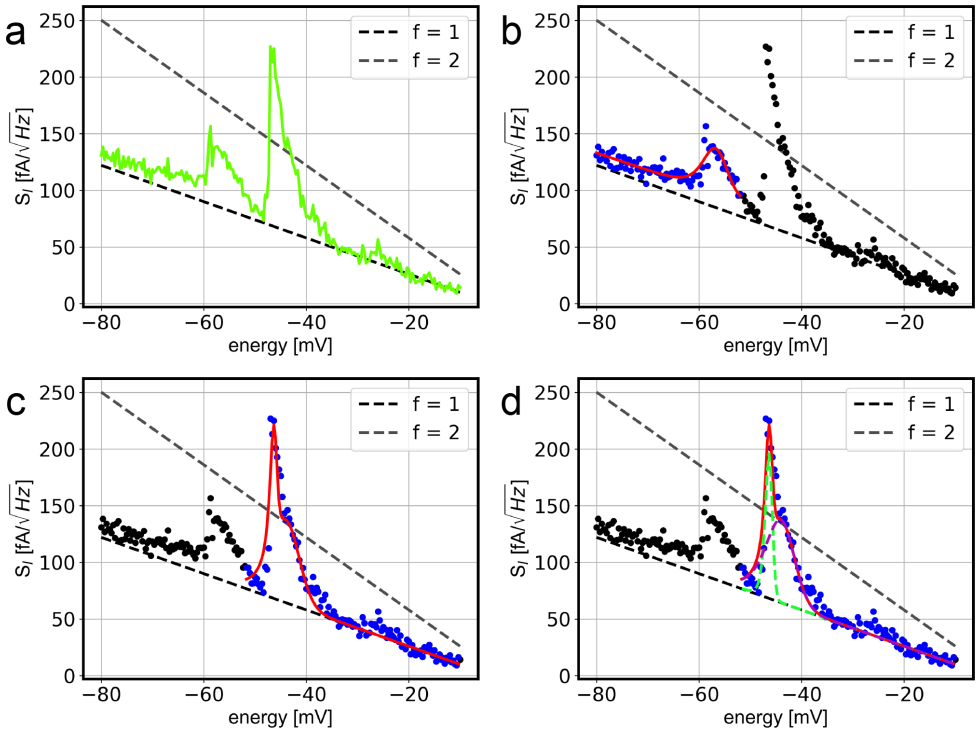

Figure 5.4: RTN and shot noise
a) Noise spectrum showing noise enhancement measured with a junction resistance of 200 MΩ. This data has previously been shown in figure 5.2b (same color). In panel (b-d) we show fits to this data with the model described in the text. In black, the measured data points are plotted. Blue markers indicate the selection of data points for fitting and the red line is the fit. Finally, in panel (d), in green and blue we demonstrate the individual components of the fitted curve. The dashed lines in each panel indicate Poissonian noise (f = 1) and doubled Poissonian noise (f = 2).

observed noise enhancement [142, 143]. However, because of the lack of any clear signature of an impurity state in the measured local DOS, we think this explanation is unlikely.
For the same reason, we believe that the observed enhancement cannot be caused by an artifact on the tip (*e.g.* a switching state). Any impurity states on the tip should be visible in the DOS measurement as well, and we furthermore see that the noise enhancement is not present homogeneously across the surface. The reason we emphasize this here is that according to our model, any source of RTN could result in the enhancement we observe. If the cluster at the apex of tip is not stable, it can switch between different configurations, effectively becoming a source of RTN itself. This can usually be observed in the tunneling current as sharp increases and decreases of the tunneling current. However, we did not observe any of these switches in the DC tunneling current, and our tip was pre-calibrated on a clean Au(111) surface where we furthermore did not see this or any noise enhancements.

5.5 Summary and outlook

In summary, we observe noise enhancements in the tunneling current when scanning a Sr_2IrO_4 sample. These appear to be highly localized, but do not appear to correlate strongly with any feature in the local DOS. The existence of substantial random telegraph noise (RTN), in addition to shot noise can explain the noise spectra we observe. Fitting our data with a model results in characteristic frequencies of ~ 100 GHz. We believe our observations indicate polaronic excitations in this iridate material, similar to noise enhancements observed in the cuprates [146]. This is intriguing and raises the question if and how Polaron- and Mott physics are related to each other in these materials.
More research is needed to substantiate these claims. A systematic study on multiple samples (with different doping levels) would give insight into whether or not these noise enhancements occur also in lower doped samples, away from the pseudogap regime where the Mott physics is supposedly stronger. Furthermore, a spatially dependent study of these noise enhancements should be done in order to learn about the exact size of the noise centers. Junction dependent measurements of the noise enhancements are also necessary, in order to learn about the dependence on the electric field emanating from the tip. This is especially relevant in light of the TIBB effect that occurs in these materials [135, 139].